HHS Public Access

Author manuscript

Proc IEEE Int Symp Biomed Imaging. Author manuscript; available in PMC 2016 October 27.

Published in final edited form as:

Proc IEEE Int Symp Biomed Imaging. 2011 ; 2011: 787–790. doi:10.1109/ISBI.2011.5872523.

SIMULATING CONVECTION-ENHANCED DELIVERY IN THE PUTAMEN USING PROBABILISTIC TRACTOGRAPHY

Do P.M. Tromp[1], **Nagesh Adluru**[1,2], **Andrew L. Alexander**[1,3,4], and **Marina E. Emborg**[4,5]

[1]Waisman Center, University of Wisconsin, Madison, WI 53715, USA

[2]Department of Biostatistics & Medical Informatics, University of Wisconsin, Madison, WI 53715, USA

[3]Department of Psychiatry, University of Wisconsin, Madison, WI 53715, USA

[4]Department of Medical Physics, University of Wisconsin, Madison, WI 53715, USA

[5]Preclinical Parkinson's Research Program, Wisconsin National Primate Research Center, University of Wisconsin, Madison, WI 53715, USA

Abstract

The treatment of brain diseases is complicated by the presence of the blood-brain barrier. This barrier limits the crossing of therapeutic molecules from the blood vessels into the brain. Today, direct intracerebral infusion applying convection-enhanced delivery (CED) is proposed to circumvent this problem and enhance the area of distribution of infusate beyond the parameters of diffusion. Several factors affect the efficacy, predictability and replicability of CED, such as the catheter model, infusion rate and site of infusion. We set out to investigate if probabilistic tractography can be used to model the infusion flow and predict the intracerebral movement of molecules. In this study we describe a modeling and analysis framework based upon probabilistic tractography. This framework was used to compare probabilistic tractography modeling and actual CED infusion measurements in the putamen of non-human primates, as this gray matter structure is proposed as a target for CED treatment of Parkinson's disease.

Keywords

Probabilistic tractography; Convection-enhanced delivery; monkeys; putamen; Parkinson's disease

1. INTRODUCTION

Parkinson's disease (PD) is a progressive neurodegenerative disorder where the main dopamine pathway in the brain, the nigrostriatal system is affected. This leads to slowing of movement, tremor at rest and stiffness. Treatment of PD is mainly focused on managing symptoms by administering dopamine precursors; there is currently no cure available for PD.

As an alternative to antiparkinsonian symptomatic treatment, neuroprotective and restorative strategies that aim to prevent, slow down and/or restore nigral cell death are been sought. Glial cell line-derived neurotrophic factor (GDNF) has emerged as a candidate treatment [1]

due to its neuroprotective and neurorestorative properties in animal models of PD [2]. The GDNF protein is unable to cross the blood-brain barrier requiring direct infusion into the brain to exert its effects. Yet clinical trials testing GDNF efficacy had controversial results and the delivery methods and target have been questioned [3,4].

Convection-enhanced delivery (CED) has been identified as a method to optimize distribution of infusate. CED increases the range of large molecules due to bulk fluid convection produced with pressure gradients [5]. CED is affected by the catheter dimension and rate of infusion. Ultimately, the architecture and geometry of the target site largely defines infusate distribution. Sophisticated models of CED are based upon the hydraulic conductivity tensor, which is typically estimated from the diffusion tensor of water in the tissue [6,7,8]. These models are complex, computationally demanding and not widely available.

It may be possible to crudely approximate the CED infusion distribution using the diffusion tensor imaging (DTI). This would be useful for target planning of infusions. Useful modeling tools must accurately predict the best target location for filling the desired region of interest (e.g., putamen, tumor) while minimizing the exposure of other brain tissues to the drug.

Recently Fonteijn *et al.* [9] proposed using probabilistic tractography to model CED infusion. A limitation of their approach was that they used a mock infusion and allowed the simulation to cross far beyond the target site.

In this study we present a framework for evaluating modeling methods for convection-enhanced delivery using both anatomical (putamen) and actual CED measurements in the nonhuman primate brain.

2. MATERIAL AND METHODS

2.1 Subjects

Eight adult macaque monkeys were obtained from the Wisconsin National Primate Center (WNPRC) and singly housed with a 12-hr light/dark cycle at the WNPRC facility (3 female and one male rhesus 6-20 yrs old, 4.2-8.9 kg; 4 female cynomolgous, 5-7 yrs old, 4.0-5.98 kg). Purina monkey chow and water was available *ad libitum*. The animals' diet was supplemented with fruit during daily enrichment. All efforts were made to ameliorate suffering of animals. This study was performed in strict accordance with the recommendations in the Guide for the Care and Use of Laboratory Animals of the National Institutes of Health. The protocol was approved by the Institutional and Animal Care Committee of the University of Wisconsin, Madison.

2.2 Infusion surgery

Following our previous published protocol [10] a pivot point-based MRI-compatible external trajectory guide (Medtronic Inc.) was set on the monkey skull under sterile conditions and isofluorane anesthesia. For the procedure the monkey was placed in a stereotaxic frame. A baseline MRI-scan provided the coordinates to locate the catheter entry

point that served as the center of a six mm diameter craniotomy. On top of it the base of the trajectory guide was secured in place using three self-tapping screws.

Multiple MRI scans were taken to aid in real-time positioning of the catheter. When on target the alignment stem was locked into position. The catheter for the infusion was threaded through the remote introducer and the guiding insert and locked into place.

The infusion was visualized with the MRI contrast agent gadoteridol (ProHance, Bracco Diagnostics; 2mMol/L). A total volume of 100μL was infused at a rate of 1μL/min.

2.3 Image acquisition

The monkeys were each scanned on a GE Discovery MR750 3T system in two separate sessions. The first session acquired a baseline MRI (T1w-BRAVO) and multiple DTI scans (EPI). Multiple diffusion scans were acquired to investigate the difference between $b = 1000ms^{-2}$ and $b = 3000ms^{-2}$. The scan sequence parameters for $b = 1000ms^{-2}$ were: TE = 71ms, TR = 6s, 42 slices and matrix of 80×80 (interpolated to 256×256 on the scanner) over a 120mm FOV, leading to 1.5mm isotropic voxels reconstructed to 0.47×0.47×1.5mm. The sequence parameters for $b = 3000ms^{-2}$ was: TE = 89.5ms, TR = 6.5s, and otherwise identical. All DTI scans measured diffusion in 55 non-collinear directions and with 10 b0 references.

On a second session the monkeys were subjected to the infusion surgery while being scanned. Images acquired included T1 (3D SPGR) scans taken at 4-minute intervals during the infusion (TE = 6ms, TR = 21ms, 64 slices and matrix of 256×256, resolution of 0.55×0.55×0.8mm).

2.4 Image analysis

To analyze the diffusion weighted images (DWI) we corrected the volumes for field inhomogeneties using the method that is described in Jezzard at al. [11]. Eddy currents in the gradient coils induce translations, stretches and shears in the diffusion weighted images. These distortions are different for different gradient directions. The DWI volumes are eddy current corrected using FSL (Oxford, UK).

We estimate the six tensor components Dxx, Dyy, Dzz, Dxy, Dxz, Dzz by non-linear optimization using a Levenburg--Marquardt algorithm. The diffusion tensor is constrained to be positive definite by fitting its Cholesky decomposition [12,13]. We use the implementation available in CAMINO [14]. Using 10 non-diffusion weighted and 55 diffusion weighted images we get high-quality estimation of the tensor components.

According to the Bose-Einstein diffusion equation:

$$\left\langle r^2 \right\rangle = 6D\Delta$$

the diffusivity measurements in [mm^2/sec] describes the mean-squared displacement of tissue water for a given diffusion time, Δ. Thus the square root of the mean squared

displacement will be proportional to the actual displacement. As an approximation to this, we compute the square root of the diffusion tensors at each voxel. The square root of a tensor is computed by eigen decomposition of the positive semi-definite tensors and reassembling the tensor by taking the square root of the eigen values. Let D denote the diffusion tensor at a voxel. Then

$$D = VEV^T$$

where E is the diagonal matrix with the eigen values and V has the eigen vectors.

$$\sqrt{D} = V \begin{bmatrix} \sqrt{e_1} & 0 & 0 \\ 0 & \sqrt{e_2} & 0 \\ 0 & 0 & \sqrt{e_3} \end{bmatrix} V^T$$

Fig. 4 shows the effect of taking the square root of the tensors especially around the putamen.

We use probabilistic tractography using the model-based PICo implementation available in CAMINO [14,15,16]. Tractography is performed iteratively each time sampling the direction in each voxel and using the tensor deflection (TEND) algorithm [17]. The probabilistic trackers use an integration of fixed step size, but the interpolation follows the method of Behrens *et al.* [18]. The tractography software was modified to stop after a specified number of steps. We use 8000 iterations per run to allow the tractography algorithm to fill the entire area. The angle threshold is set at 180 degrees. For each tractography the number of steps are run between 5 and 50.

We seed the PICo tractography close to the infusion target point and estimate mean connection probability index of all other voxels to this seed voxel. The output of each run was compared to CED infusion at two time points, an early time point with a smaller CED volume and later time point with a larger CED infusion volume.

After determining the optimal parameters we used these to investigate multiple seed locations in a single monkey. Eighteen seed points were placed on two separate slices in the putamen area, as illustrated in Fig. 1. The putamen area was then masked and used to determine the optimal infusion seed. We compared this data to the CED infusion.

3. RESULTS

To evaluate the quality of our simulation in predicting actual infusion patterns we characterized the overlap of the tractography with the measured CED infusion distribution using the metrics precision and recall [19], defined as:

$$\text{Precision} = \frac{tp}{tp+fp}$$
$$\text{Recall} = \frac{tp}{tp+fn}$$

where *tp* is the true positive, *fp* the false positive and *fn* the false negative. The Precision describes the fraction of voxels inside the desired target area. The Recall describes the fractional efficiency of filling the target area. Both measures are highly desirable for this problem. To determine the harmonic mean of precision and recall we used the balanced F-measure:

$$F=2\cdot\frac{\text{precision}\cdot\text{recall}}{\text{precision}+\text{recall}}$$

The F-measure was used to establish the local optimum depending on what parameters were applied. Results showed that optimal parameters were equal for both small and big CED infusions. The best performance was achieved when applying the square root of the tensors at $b = 1000s/mm^2$. The simulation of the small infusion peaked after 10 steps, and the large infusion after 15 steps. Results are shown in Fig. 2.

This information was then used to run tractography of multiple seed points on a single brain. Output showed that seed location number 7 produced the most optimal overlap with the putamen mask; this optimum was achieved after 20 steps (Fig. 3). This seed location is about 0.7mm more medial and inferior compared to the seed location used for the CED infusion. The putamen mask and optimal tractography from seed 7 are visualized and compared to the actual CED infusion in Fig. 5.

4. DISCUSSION AND CONCLUSION

This paper set out to describe a framework for assessing models that simulate CED infusion. In this study we compared CED infusion images to tractography simulations using multiple scan acquisitions and a new algorithm to calculate the square root of tensors. Results indicated that scanning DTI images at $b = 1000s/mm^2$ shows slightly better results, while taking the square root of the tensor greatly improved the simulation.

Next, the optimal parameters were used to investigate what seed location would produce tractography maps that showed the best overlap with the putamen. The optimal seed for the putamen mask was more medial and inferior than the seed used in the actual infusion, which might explain the slightly lateral location of the infusion.

The probabilistic tractography method showed a pattern of filling in three dimensions, which is consistent with primarily isotropic diffusion properties in the putamen. The resultant pattern yielded modest overlap with the actual CED infusion distribution that was measured in the same brains. It should be noted that the current tractography mapping approach does not scale with the actual diffusivities of the diffusion tensor as the tensor dimensions are normalized prior to tractography.

Other factors may improve the CED modeling further -- resampling the data to isotropic voxels, using a different tractography algorithm, higher order diffusion models and decreasing the step size with each new step to better mimic diffusion processes.

Our probabilistic tractography approach initially used an approach similar to that described by Fonteijn *et al.* [9]; however, we found that their probabilistic tractography approach yielded extremely poor precision in predicting the CED infusion pattern. The refinements to the modeling technique as outlined significantly improved the accuracy. However, despite these improvements, the current performance is not likely adequate for predicting CED infusions with high accuracy and thus this should be considered a work-in-progress.

ACKNOWLEDGEMENTS

This research was supported in part by the Kinetics Foundation, NIH MH62015 and the Grant P51 RR000167 from the NIH-NCRR to the WNPRC University of Wisconsin-Madison and a CIBM-MIR fellowship.

REFERENCES

[1]. Lin LF, Doherty DH, Lile JD, Bektesh S, et al. GDNF: a glial cell line-derived neurotrophic factor for midbrain dopaminergic neurons. Science. May.1993 :1130–1132.

[2]. Kiri D, Georgievska B, Björklund A. Localized striatal delivery of GDNF as a treatment for Parkinson disease. Nature Neuroscience. 2004:105–110. [PubMed: 14747832]

[3]. Sherer TB, Fiske BK, Scendsen CN, Lang AE, Langston JW. Crossroads in GDNF therapy for Parkinson's disease. Mov Disord. Feb.2006 :136–141. [PubMed: 16470786]

[4]. Morrison PF, Lonser RR, Oldfield EH. Convective delivery of glial cell line-derived neurotrophic factor in the human putamen. J Neurosurg. Jul.2007 :74–83.

[5]. Bobo RH, Laske DW, Akbasak A, et al. Convection-enhanced delivery of macromolecules in the brain. Proc. Natl. Acad. Sci. U.S.A. Mar.1994 :2076–2080. [PubMed: 8134351]

[6]. Linninger AA, Somayaji MR, Zhang L, et al. Rigorous mathematical modeling techniques for optimal delivery of macromolecules to the brain. IEEE Trans Biomed Eng. Sep.2008 :2303–13. [PubMed: 18713700]

[7]. Sarntinoranont M, Chen X, Zhao J, Mareci TH. Computational model of interstitial transport in the spinal cord using diffusion tensor imaging. Ann Biomed Eng. Aug.2006 :1304–21. [PubMed: 16832605]

[8]. Raghavan R, Brady ML, Rodríguez-Ponce MI, et al. Convection-enhanced delivery of therapeutics for brain disease, and its optimization. Neurosurg Focus. Apr 15.2006 20(4):E12. [PubMed: 16709017]

[9]. Fonteijn HM, Woodhouse M, White E, et al. Determining infusion sites for Convection Enhanced Delivery using probabilistic tractography. MICCAI 2010 CDMRI. 2010:156–164.

[10]. Emborg ME, Joers V, Fisher R, et al. Intraoperative intracerebral MRI-guided navigation for accurate targeting in nonhuman primates. Cell Transplantation. 2010

[11]. Jezzard, Peter; Clare, Stuart. Sources of distortion in functional MRI data. Human Brain Mapping. 1995:80–85.

[12]. Jones DK, Basser PJ. Squashing peanuts and smashing pumpkins: How noise distorts diffusion-weighted MR data. Magnetic Resonance in Medicine. 2004:979–993. [PubMed: 15508154]

[13]. Alexander DC, Barker GJ. Optimal imaging parameters for fibre-orientation estimation in diffusion MRI. NeuroImage. 2005:357–367. [PubMed: 15921931]

[14]. Cook, PA.; Bai, Y.; Nedjati-Gilani, S., et al. Camino: Open-Source Diffusion-MRI Reconstruction and Processing; 14th Scientific Meeting of the ISMRM; 2006; p. 2759

[15]. Parker GJM, Haroon HA, Wheeler-Kingshott CAM. A framework for a streamline-based Probabilistic Index of Connectivity (PICo) using a structural interpretation of MRI diffusion measurements. Journal of Magnetic Resonance Imaging. 2003:242–254. [PubMed: 12884338]

[16]. Cook PA, Alexander DC, Parker GJM. Modelling noise-induced fibre-orientation error in diffusion-tensor MRI. IEEE ISBI. 2004:332–335.

[17]. Lazar M, Weinstein DM, Tsuruda JS, et al. White matter tractography using diffusion tensor deflection. Human Brain Mapping. 2003:306–321. [PubMed: 12632468]

[18]. Behrens TEJ, Woolrich MW, Jenkinson M, et al. Characterization and propagation of uncertainty in diffusion-weighted MR imaging. Magnetic Resonance in Medicine. 2003:1077–1088.

[19]. Olson, DL.; Delen, D. Advanced Data Mining Techniques. 1 edition. Springer; Feb 1. 2008 p. 138ISBN 3540769161

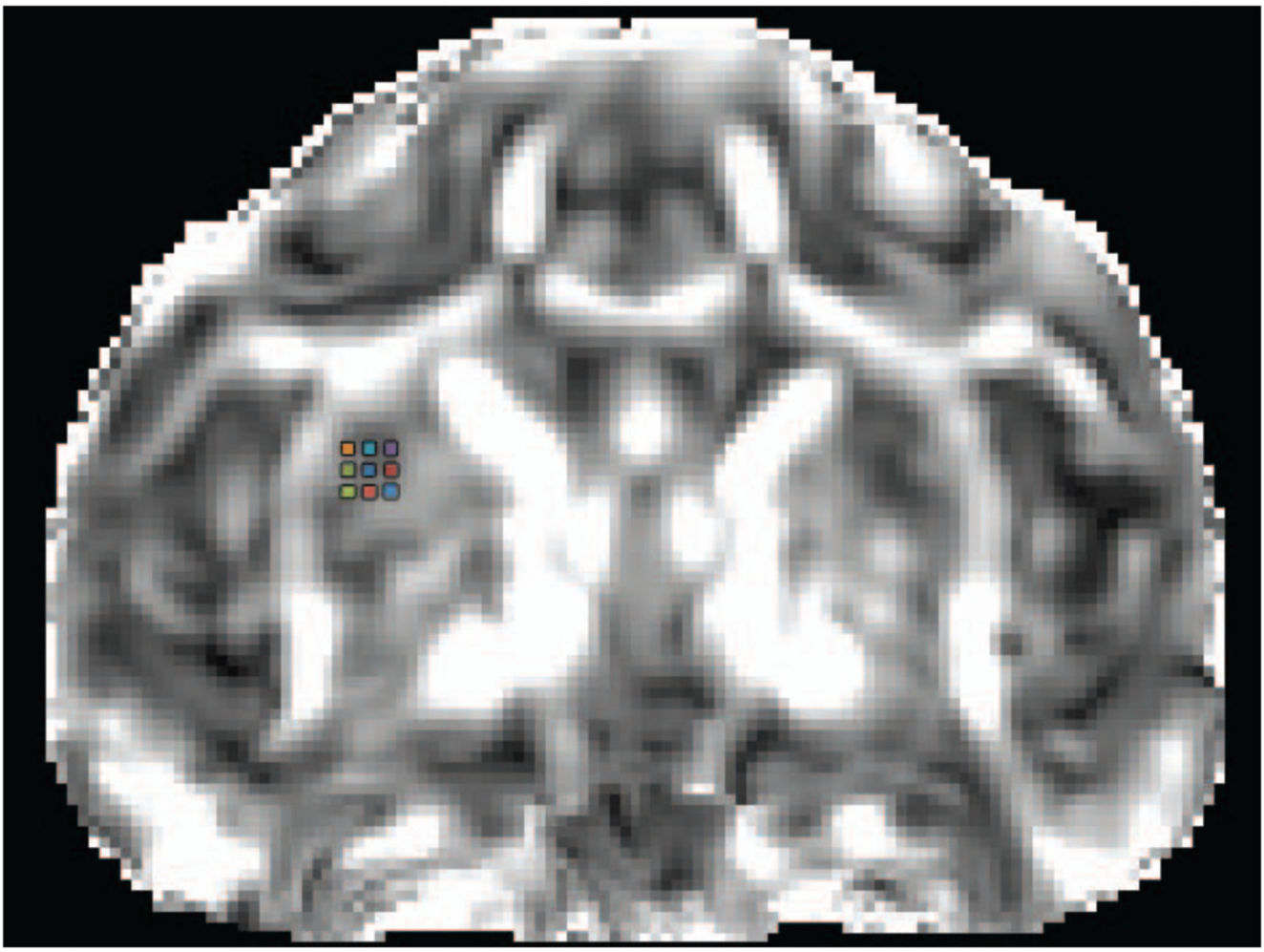

Figure 1.
Nine seed points visualized on the FA map

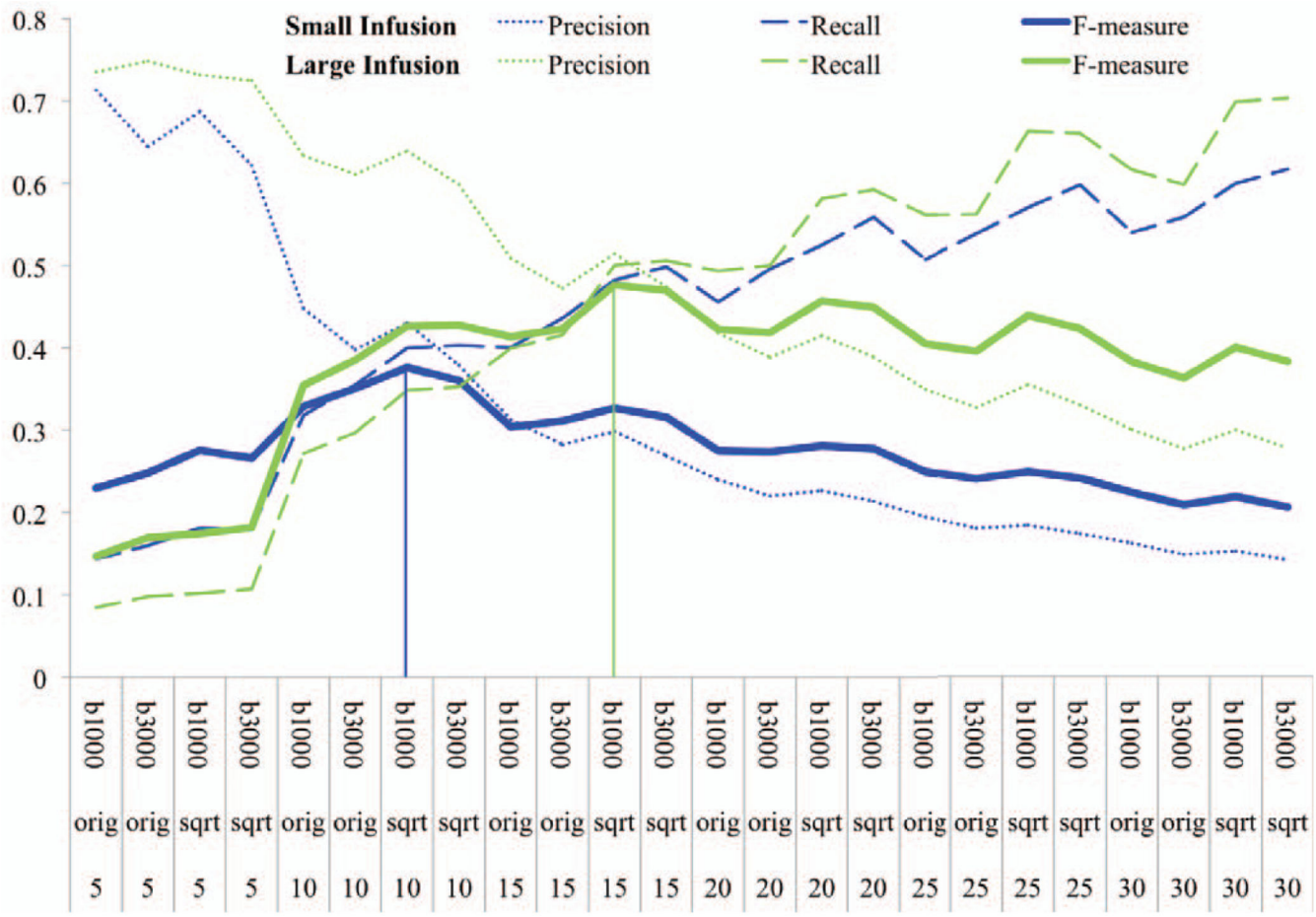

Figure 2.

Precision, Recall and F-measure of the small CED infusion (in blue) and bigger CED infusion (in green). Vertical lines indicate local optima. The x-axis shows the applied parameters

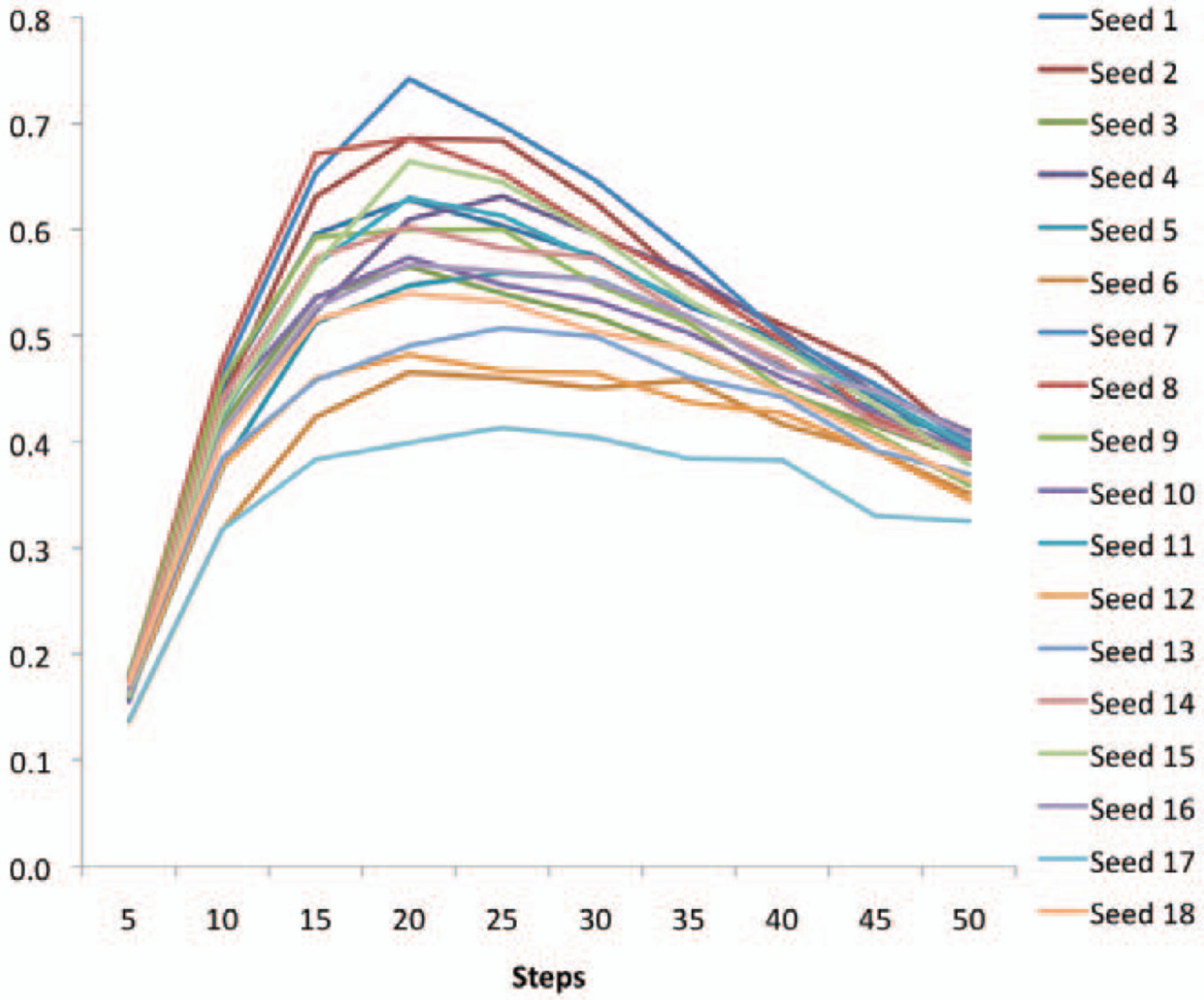

Figure 3.
F-measure for putamen mask per seed

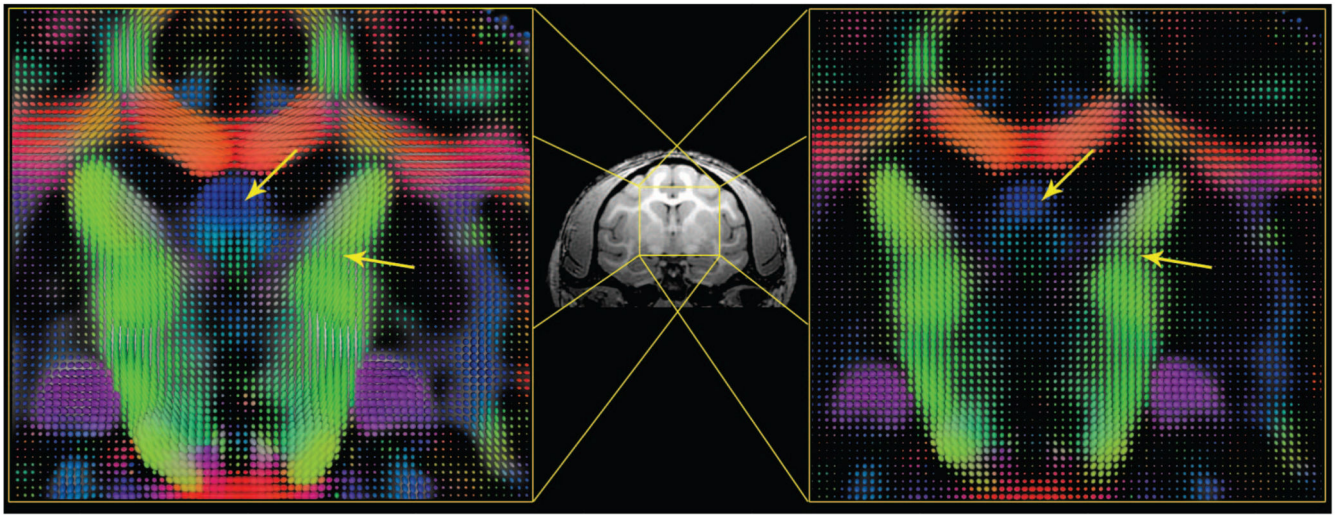

Figure 4.
Glyph representation of tensors, left is before taking the square root, right after. Arrows indicate areas with clear changes

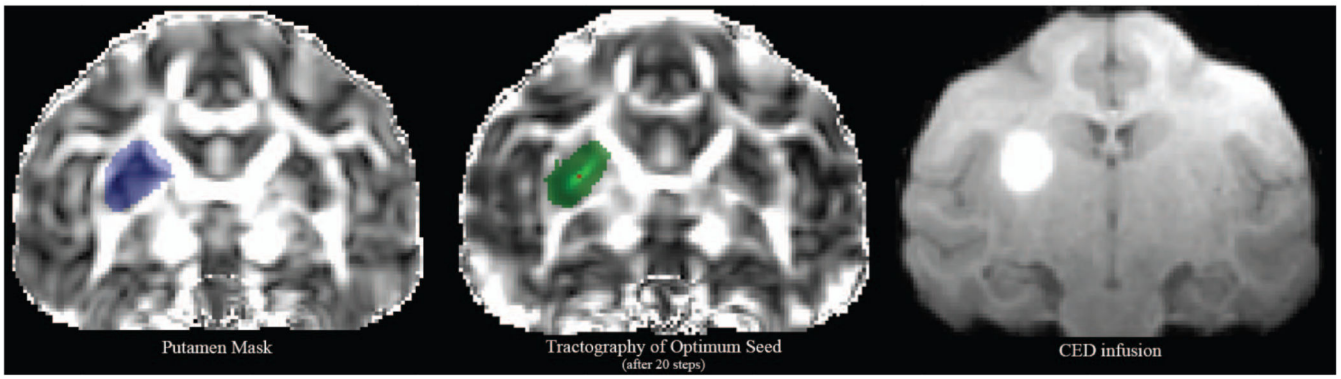

Figure 5.

Visualization of putamen mask (left image in blue) and tractography of optimum seed (middle image in green, with in red the location of the seed) overlaid on the FA mask. The right image shows the actual CED infusion